J|A|C|S
COMMUNICATIONS

d^8 Rhodium and Iridium Complexes of Corannulene

Jay S. Siegel,* Kim K. Baldridge, Anthony Linden, and Reto Dorta*

Institute of Organic Chemistry, University of Zurich, Winterthurerstrasse 190, CH-8057 Zurich, Switzerland

Received March 28, 2006; E-mail: jss@oci.unizh.ch; dorta@oci.unizh.ch

Compared with the wealth of reported metal binding to C_{60} and its derivatives,[1] metal coordination to corannulene ($C_{20}H_{10}$), the curved carbon fragment of buckminsterfullerene, is rare at present.[2] To date, stable corannulene metal complexes display an η^6 bond to the carbon atoms of the six-membered rings, with the metal fragments having the formula [Cp*M] (Cp* = η^5-C_5Me_5, M = Ru^+, Ir^{2+}).[3,4] Unfortunately, such [Cp*M] fragments are extremely stable and therefore preclude any chemistry beyond complexation/decomplexation of corannulene.

The synthesis of d^8 metal complexes of corannulene proceeds facilely starting from labile, cationic Rh(I) and Ir(I) precursors of formula $[(COE)_2M(acetone)_2]PF_6$ (M = Rh (**1**),[5] Ir (**2**);[6] COE = cyclooctene). Treatment of unsaturated **1** and **2** with an equimolar amount of corannulene at room temperature in a diethyl ether suspension leads to substitution of the acetone ligands and to a slight color change of the slurry from yellow−orange to yellow (eq 1). After 12 h, the precipitates were washed and dried in vacuo to give the η^6 complexes $[(COE)_2Rh(\eta^6\text{-}C_{20}H_{10})]PF_6$ (**3**) and $[(COE)_2Ir(\eta^6\text{-}C_{20}H_{10})]PF_6$ (**4**) in quantitative yield.

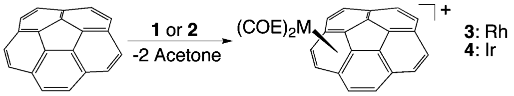

(1)

In the crystal structures of **3** (Figure 1) and **4** the $[(COE)_2M]^+$ units are η^6-coordinated to the exo side of corannulene, as observed in the other known structure, $[Cp^*Ru(\eta^6\text{-}C_{20}H_{10})]SbF_6$.[3e] The bond distances between the η^6-coordinated ring carbon atoms and the metal atom range from 2.24 to 2.57 Å, with the shortest involving the rim atoms (C7, C8) and the longest involving the spoke atoms C6 and C9. The formally η^6-bonded ring has a shallow boat geometry. The average M−C_{ring} distances for **3** (2.40 Å) and **4** (2.38 Å) are substantially longer than those found for the ruthenium complex (Ru−C_{av} 2.27 Å). Bond distances greater than 2.5 Å (M−C9) are unusual for η^6-coordinated aromatic molecules.

Although some complexes of general formula $[(COE)_2M(\eta^6\text{-arene})]^+$ have been reported, the absence of crystal structure data precludes comparisons with **3** and **4**. The known complexes $[(COE)_2Rh(\eta^6\text{-}C_6H_6)]PF_6$ (**5**) and $[(COE)_2Ir(\eta^6\text{-}C_6H_6)]PF_6$ (**6**),[7] as well as the new phenanthrene complexes $[(COE)_2Rh(\eta^6\text{-}C_{14}H_{10})]PF_6$ (**7**) and $[(COE)_2Ir(\eta^6\text{-}C_{14}H_{10})]PF_6$ (**8**), were prepared in high yield by following the procedure used for **3** and **4**.[8] Their crystal structures (see Supporting Information) as well as in situ NMR studies show that complexation of $[(COE)_2M]^+$ to phenanthrene occurs exclusively at the peripheral ring. The average M−C_{ring} distances increase from **5** (2.32 Å) to **7** (2.36 Å) to **3** (2.40 Å) for the Rh series and from **6** (2.30 Å) to **8** (2.33 Å) to **4** (2.38 Å) for the Ir compounds; the Rh series consistently shows longer distances than Ir, although both covalent and ionic radii of the former are smaller. It clearly indicates tighter binding of the third-row metal to planar as well as curved aromatics.

The metal atom in **7** and **8** is nearly 0.2 Å further from the carbon atoms connected to the condensed central ring than from the remaining C_{ring} atoms. This latter observation explains the binding selectivity in the phenanthrene compounds (no coordination of M to the central ring) and may also account for the long distances in the corannulene metal complexes, where the metal binding site is connected to three additional aromatic rings.

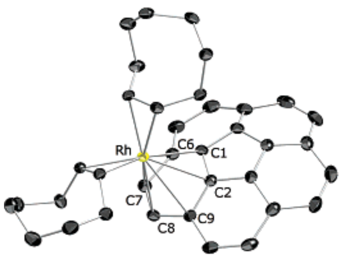

	3	4
M-C1	2.385(4)	2.366(3)
M-C2	2.453(4)	2.409(3)
M-C6	2.472(3)	2.488(3)
M-C7	2.239(3)	2.234(3)
M-C8	2.262(3)	2.246(4)
M-C9	2.567(3)	2.537(3)

Figure 1. ORTEP drawing (50% probability) of $[(COE)_2Rh(\eta^6\text{-}C_{20}H_{10})]^+$ (cation **3**, left) and selected bond lengths (Å) for **3** and **4** (right).

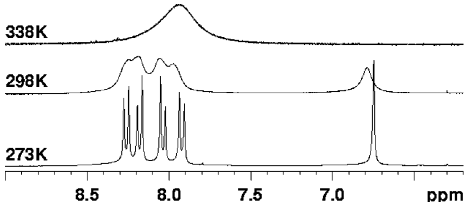

Figure 2. Variable temperature ^1H NMR spectra of **3**.

The ^1H NMR spectrum of **3** at 298 K (in CD_2Cl_2, $C_2D_2Cl_4$, or CD_3NO_2) displays broad signals in the aromatic region, whereas distinct resonances for all of the protons of corannulene were obtained at lower temperature (273 K), showing one singlet for the aromatic ring bound to the metal (δ 6.75) and four doublets for the remaining protons at δ 7.92 (J = 9.0 Hz), 8.04 (J = 8.8 Hz), 8.18 (J = 8.8 Hz), and 8.26 (J = 9.0 Hz). Coalescence to a single broad resonance at δ 7.94 occurs at 338 K without decomposition of **3** (Figure 2). To establish the nature of the fluxionality in **3**, VT experiments with added COE (5 equiv) as well as in the presence of excess corannulene (0.5 equiv) were carried out. Both these control experiments did not influence the fluxionality in **3** and strongly suggest inter-ring movement of the $[(COE)_2Rh]^+$ fragment over the curved aromatic surface of corannulene.[9] Whereas such haptotropic shifts have been seen in other aromatic networks, they normally either need higher temperatures and/or are catalyzed by intermittent binding of polar solvent molecules to the metal center.[10]

The inter-ring movement of $[(COE)_2Rh]^+$ might occur by one of two distinct mechanisms (Scheme 1). Either the metal fragment follows the outer edge of corannulene and migrates from one arene ring to the next via a $\eta^6 \rightarrow \eta^4(\eta^2) \rightarrow \eta^6$ mechanism (rim migration), or the migration occurs by walking over the central five-membered ring in a $\eta^6 \rightarrow \eta^5 \rightarrow \eta^6$ process (hub migration).

The 2D EXSY NMR spectrum of complex **3** at 278 K displayed cross-peaks between the singlet of the η^6-metal-coordinated ring and all of the other four aromatic ring signals at long mixing times

10.1021/ja062110x CCC: $33.50 © 2006 American Chemical Society

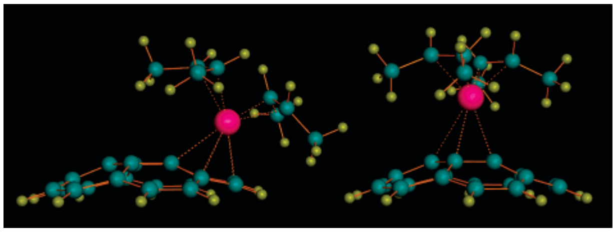

Figure 3. Calculated structures for [(2-butene)$_2$Rh(η^6-$C_{20}H_{10}$)]$^+$ (left) and [(2-butene)$_2$Rh(η^5-$C_{20}H_{10}$)]$^+$ (right).

Scheme 1. Possible Metal Migration Mechanisms in **3**

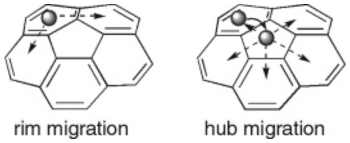

(500 ms), whereas at 3 μs, no exchange occurred. Variation of the mixing time between 3 μs and 500 ms showed a rapid onset of cross-peaks among all signals between 1 and 5 ms, without distinction between vicinal and distal C_6 fragments. This speaks against a rim migration, strongly favoring the hub migration mechanism.

Indirect evidence supporting the feasibility of η^5 binding to [(COE)$_2$Rh]$^+$ comes from complexation of **1** to the electron-rich C_5 fragment of azulene to give [(COE)$_2$Rh(η^5-$C_{10}H_8$)]PF$_6$ (**9**), which shows strong metal binding to azulene in the crystal structure (see Supporting Information).

Hybrid DFT calculations provide a model for understanding the structure and dynamics of **3** and **4** (Figure 3).[11] The minimum structure for both complexes locates the metal over a six-membered ring, with a ligand field arrangement, bowl structure, boat geometry, and relative bond lengths consistent with those in the crystal structures. A second minimum higher in energy (Rh, 3.5, and Ir, 5.2 kcal/mol) is predicted for the metal over the five-membered ring. To the extent intermediate energies reflect activation energies, these computations predict the dynamics in **4** to be substantially slower than those in **3**.

As inferred from the HDFT computations and suggested by the shorter M$-$C$_{\text{ring}}$ distances in the solid state, **4** does not show the fluxionality observed for **3**. The ^{1}H NMR spectrum at 298 K gives sharp signals for the aromatic protons of corannulene, and no cross-peaks are observed in the 2D EXSY NMR experiment. However, **4** undergoes a transformation upon heating at 80 °C that gives rise to a new set of aromatic signals and additional resonances at δ 4.72 (s) and ca. 2.1 (m), which indicate the formation of [(COD)-Ir(η^6-$C_{20}H_{10}$)]PF$_6$ (**10**, COD = cyclooctadiene). Independent synthesis of **10** from [(COD)Ir(μ^2-Cl)]$_2$, AgPF$_6$, and $C_{20}H_{10}$ confirmed its identity (see Supporting Information). As expected, dehydrogenation of one COE ligand of **4** is accompanied by generation of cyclooctane (COA), as seen from a growing signal at δ 1.50 (s) and a GC/MS analysis of the reaction mixture.[12]

In situ formation of **10** from complex **4** highlights the fact that these [(COE)$_2$M]$^+$ fragments can undergo chemical transformations while still bound to corannulene. In a related example, low-temperature addition of 1 equiv of P^{i}Pr$_3$ to **3** in CD$_2$Cl$_2$ selectively substitutes one COE to give [(COE)(P^{i}Pr$_3$)Rh(η^6-$C_{20}H_{10}$)]PF$_6$ (**11**). The ^{31}P{^{1}H} NMR spectrum shows a doublet at δ 59.3 (J = 174.9 Hz) with ^{1}H NMR signals of P^{i}Pr$_3$ at δ 0.84 (dd) and 1.48 (m). A shoulder at δ 6.6 and a broad signal at δ 8.06 indicate more facile migration of **10** than of **3** over the corannulene surface. Coalescence to a single broad resonance occurs at 313 K, whereas distinct proton signals are seen at 253 K. The marginally longer M$-$C$_{\text{ring}}$ distances in the crystal structure of **11** (see Supporting Information) are in accord with the higher fluxionality in solution. Changing ancillary ligation by varying the [L$_2$M]$^+$ fragments should provide valuable insights into the binding characteristics of curved surfaces of corannulene and its derivatives. These compounds will also allow a more detailed investigation of the factors governing metal migration over curved aromatic networks.

Scheme 2. Reactivity of the [(COE)$_2$M]$^+$ Fragment in **3** and **4**

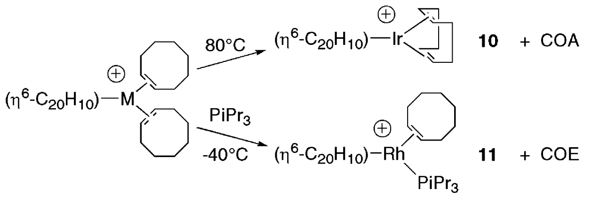

Acknowledgment. R.D. is the recipient of an Alfred Werner Assistant Professorship and thanks the foundation for generous financial support. We thank Nadja Bross and Simon Jurt for NMR assistance. J.S.S., K.K.B., and R.D. thank the Schweizerische Nationalfonds for support.

Supporting Information Available: Experimental and computational procedures and CIFs for **3**−**9** and **11**. This material is available free of charge via the Internet at http://pubs.acs.org.

References

(1) Lee, K.; Song, H.; Park, J. T. *Acc. Chem. Res.* **2003**, *36*, 78 and references therein.
(2) A recent investigation even claims that common routes leading to metal complexation of planar aromatic hydrocarbons fail in the case of corannulene: Stoddart, M. W.; Brownie, J. H.; Baird, M. C.; Schmider, H. L. *J. Organomet. Chem.* **2005**, *690*, 3440.
(3) (a) Seiders, T. J.; Baldridge, K. K.; O'Connor, J. M.; Siegel, J. S. *J. Am. Chem. Soc.* **1997**, *119*, 4781. (b) Seiders, T. J.; Baldridge, K. K.; O'Connor, J. M.; Siegel, J. S. *Chem. Commun.* **2004**, 950. (c) Alvarez, C. M.; Angelici, R. J.; Sygula, A.; Sygula, R.; Rabideau, P. W. *Organometallics* **2003**, *22*, 624. (d) Vecchi, P. A.; Alvarez, C. M.; Ellern, A.; Angelici, R. J.; Sygula, A.; Sygula, R.; Rabideau, P. W. *Angew. Chem., Int. Ed.* **2004**, *43*, 4497. (e) Vecchi, P. A.; Alvarez, C. M.; Ellern, A.; Angelici, R. J.; Sygula, A.; Sygula, R.; Rabideau, P. W. *Organometallics* **2005**, *24*, 4543.
(4) η^2 complexes of Rh(II) and Ag(I) have been reported but are not stable in solution: (a) Petrukhina, M. A.; Andreini, K. W.; Mack, J.; Scott, L. T. *Angew. Chem., Int. Ed.* **2003**, *42*, 3375. (b) Elliott, E. L.; Hernandez, G. A.; Linden, A.; Siegel, J. S. *Org. Biomol. Chem.* **2005**, *3*, 407.
(5) Windmüller, B.; Nürnberg, O.; Wolf, J.; Werner, H. *Eur. J. Inorg. Chem.* **1999**, 613.
(6) Dorta, R.; Rozenberg, H.; Shimon, L. J. W.; Milstein, D. *J. Am. Chem. Soc.* **2002**, *124*, 188.
(7) Schrock, R. R.; Osborn, J. A. *J. Am. Chem. Soc.* **1971**, *93*, 3089.
(8) Synthetic details will be reported elsewhere.
(9) In the VT experiments with added corannulene, slight broadening of the signal for free corannulene above 333 K indicates that a parallel, dissociative mechanism might also operate at these high temperatures.
(10) Nambu, M.; Baldridge, K. K.; Mohler, D.; Hardcastle, K.; Siegel, J. S. *J. Am. Chem. Soc.* **1993**, *115*, 6138 and references therein.
(11) Computation: B3LYP[11a] and MP2[11b] methods using GAMESS[11c] and Gaussian[11d] relativistic double-ζ effective core potentials SDD[11e] and LANL2DZ[11f,g] were used for transition metals; all other atoms employed Dunning/Huzinaga double-ζ basis set.[11g] (a) Becke, A. D. *J. Chem. Phys.* **1993**, *98*, 5648. (b) Moller, C.; Plesset, M. S. *Phys. Rev.* **1934**, *46*, 618. (c) Schmidt, M. W.; Baldridge, K. K.; Boatz, J. A.; Elbert, S. T.; Gordon, M. S.; Jensen, J. H.; Koseki, S.; Matsunaga, N.; Nguyen, K. A.; Su, S.; Windus, T. L.; Elbert, S. T. *J. Comput. Chem.* **1993**, *14*, 1347. (d) Frisch, M. J.; et al. *Gaussian 98*; Gaussian, Inc.: Pittsburgh, PA, 1998. (e) Fuentealba, P.; Preuss, H.; Stoll, H.; Szentpaly, L. v. *Chem. Phys. Lett.* **1989**, *89*, 418. (f) Hay, P. J.; Wadt, W. R. *J. Chem. Phys.* **1985**, *82*, 270. (g) Dunning, T. H., Jr.; Hay, P. J. In *Modern Theoretical Chemistry*; Schaefer, H. F., III, Ed.; Plenum: New York, 1976; Vol. 3, p 1.
(12) For dehydrogenation of COE on a similar Ir(I) center, see: Bernskoetter, W. H.; Lobkovsky, E.; Chirik, P. J. *Organometallics* **2005**, *24*, 6250.

JA062110X